1. James, W. *The Principles of Psychology* (Holt, New York, 1890).
2. Gold, P.E. & McGaugh, J.L. in *Short-Term Memory* (eds Deutsch, D. & Deutsch, J.A.) 355–378 (Academic, New York, 1975).
3. Izquierdo, I. & Medina, J.H. *Neurobiol. Learn. Mem.* **68,** 285–316 (1997).
4. Squire, L.R., Knowlton, B. & Musen, G. *Annu. Rev. Psychol.* **44,** 453–495 (1993).
5. Rosenzweig, M.R. *et al. Behav. Brain Res.* **57,** 193–198 (1993).
6. Izquierdo, I. *et al. Eur. J. Neurosci.* **9,** 786–793 (1997).
7. Bevilaqua, L. *et al. Behav. Pharmacol.* **8,** 331–338 (1997).
8. Bernabeu, R. *et al. Proc. Natl Acad. Sci. USA* **94,** 7041–7046 (1997).
9. Paxinos, G. & Watson, C. *The Rat Brain in Stereotaxic Coordinates* (Academic, San Diego, 1986).
10. Izquierdo, I. *et al.* in *Monoamine Interactions and Brain Disease* (eds Palamo, T., Archer, R. & Beninger, R.) (Farrand, London, in the press).
11. Martin, J.H. *Neurosci. Lett.* **127,** 160–164 (1991).

Walking on Mars

Sometime in the near future humans may walk in the reduced gravity of Mars. Gravity plays an essential role in walking. On Earth, the body uses gravity to 'fall forwards' at each step and then the forward speed is used to restore the initial height in a pendulum-like mechanism. When gravity is reduced, as on the Moon or Mars, the mechanism of walking must change[1]. Here we investigate the mechanics of walking on Mars onboard an aircraft undergoing gravity-reducing flight profiles. The optimal walking speed on Mars will be 3.4 km h^{-1} (down from 5.5 km h^{-1} on Earth) and the work done per unit distance to move the centre of mass will be half that on Earth.

In contrast to swimming or flying, during which the fins or wings can slide against the surrounding medium, locomotion on a solid surface is constrained by the link between the centre of gravity of the body and the fixed point of contact of the foot on the ground. After foot contact, this link leads to a forward deceleration which must be compensated for by a subsequent forward acceleration in order to maintain a constant average speed of locomotion. This increases the cost of terrestrial locomotion.

However, this cost is contained by the transfer of kinetic energy into gravitational potential energy during the deceleration (when the body rides upwards on the leg after heel strike) and the subsequent recovery of kinetic energy from the potential energy during acceleration. The recovery of mechanical energy by this mechanism is described by

$$R = (W_f + W_v - W_{cm})/(W_f + W_v)$$

where W_f is the work needed to increase the kinetic energy, W_v is the work to increase the potential energy, and W_{cm} is the work to increase the total mechanical energy of the centre of mass. With an ideal, frictionless pendulum, W_{cm} would be nil and R equal to 1. With walking on Earth, R attains a maximum of 0.7 at about 5.5 km h^{-1} (Fig. 1) near the speed at which the energy expenditure per unit distance is at a minimum[2]. At higher and lower speeds, R decreases and the energy cost increases.

We investigate the mechanics of locomotion on Mars in three male subjects (of weight and height, respectively, of 77 kg, 1.79 m; 92 kg, 1.93 m; 86 kg, 1.79 m) walking at different speeds in a Martian gravity (0.4*g*, maintained for about 30 s) on a force platform (3 m × 0.4 m) sensitive to the force exerted in both forward and vertical directions[3]. The platform was fixed to the floor of a KC-135 and an A300 Airbus aeroplane during the 23rd and 24th European Space Agency parabolic flight campaigns. The force signals from the plate (also measured in ref. 4) were analysed[5] to determine W_{cm} and R.

Figure 1 shows that on Mars the maximum pendular recovery of mechanical energy R is reduced to 0.6 and occurs at the lower speed of 3.4 km h^{-1}. In spite of the lower R, the minimum mechanical work done per unit distance to maintain the motion of the centre of mass on Mars is about one half of that on Earth. In general, walking a given distance at any absolute speed will be cheaper on Mars than on Earth. In fact, the energy consumption measured during locomotion in simulated partial gravity is less than that at 1*g* (refs 6,7). A decrease in the maximum speed of walking was also observed in partial gravity simulators[7,8].

On Mars, then, both the optimal walking speed and the range of possible walking speeds will be about half those on Earth. The walk–run transition on Mars will occur near the optimal walking speed on Earth, and the mechanical work done to walk a given distance on Mars will be about half of what it would be on Earth. So, energy expenditure will probably be lower and locomotion smoother on Mars.

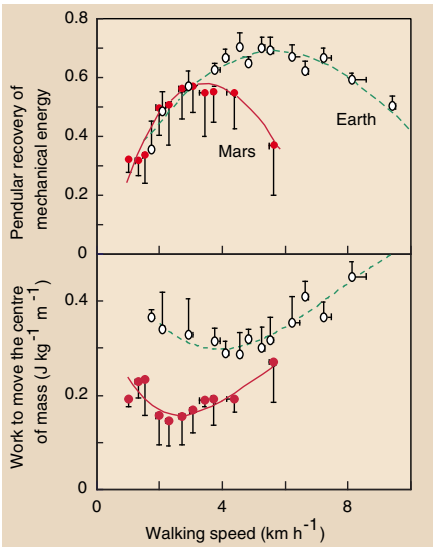

Figure 1 Comparison of the mechanics of walking on the Earth and on Mars. Top, mechanical energy recovered during walking by the pendular transfer between potential energy and kinetic energy of the centre of mass of the body on Mars and on Earth. Bottom, the work required to maintain the movement of the centre of mass in a sagittal plane. Note that the range of walking speeds on Mars is about half that on Earth (data on Earth were obtained from earlier studies on the same subjects[9,10]). Mars, filled circles; Earth, open circles.

G. A. Cavagna
Istituto di Fisiologia Umana, Università di Milano, 20133 Milan, Italy
e-mail: cavagna@imiucca.csi.unimi.it
P. A. Willems, N. C. Heglund
Unité de Réadaptation, Université Catholique de Louvain, 1348 Louvain-la-Neuve, Belgium

1. Margaria, R. & Cavagna, G. A. *Aerospace Med.* **35,** 1140–1146 (1964).
2. Cavagna, G. A., Thys, H. & Zamboni, A. *J. Physiol., Lond.* **262,** 639–657 (1976).
3. Heglund, N. C. *J. Exp. Biol.* **93,** 333–338 (1981).
4. Rajulu, S. L., Klute, G. K. & Moore, N. R. *SAE Tech. Pap. Ser.* 22nd Intl Conf. on Environmental Systems, Seattle (1992).
5. Cavagna, G. A. *J. Appl. Physiol.* **39,** 174–179 (1975).
6. Farley, C. T. & McMahon, T. A. *J. Appl. Physiol.* **73,** 2709–2712 (1992).
7. Newman, D. J., Alexander, H. L. & Webbon, B. W. *Aviat. Space Envir. Med.* **65,** 815–823 (1994).
8. Hewes, D. E., Spady, A. A. Jr & Harris, R. L. *NASA Techn. Note* TND-3363 (1966).
9. Cavagna, G. A., Franzetti, P. & Fuchimoto, T. *J. Physiol., Lond.* **343,** 323–339 (1983).
10. Willems, P. A., Cavagna, G. A. & Heglund, N. C. *J. Exp. Biol.* **198,** 379–393 (1995).

Relations of the new phylum Cycliophora

The Cycliophora is the most recently described animal phylum and is based on a single species, *Symbion pandora*, which was discovered on the mouthparts of the Norway lobster *Nephrops norvegicus*[1]. Because only a few morphological data[1–3] are available for *Symbion*, the precise nature of its phylogenetic relationships is highly controversial[2,4,5]. Here we present a phylogenetic analysis of 18S ribosomal RNA sequence data, including a new *Symbion* sequence, which places *Symbion* in a lophophorate–aschelminth–protostome clade and which suggests a sister-group relationship between Cycliophora and a Rotifera–Acanthocephala clade.

N. norvegicus with attached *S. pandora* were collected in Kosterfjord, Sweden. We used the polymerase chain reaction to amplify 18S rRNA gene sequences from alcohol-preserved animals, and then used standard sequencing techniques to obtain 1,542 base pairs (bp) and 1,858 bp of the 18S rRNA gene sequences from *S. pandora* (EBI number Y14811) and *N. norvegicus* (Y14812), respectively. We added the sequences to an 18S rRNA database[6]. We used four tree-construction methods and

assessed the stability of the phylogenetic trees using bootstrapping (100 or 1,000 samples), confidence probability[7] calculations and decay index[8] calculations.

A neighbour-joining analysis of 18S rRNA sequences from a broad range of metazoan taxa placed *Symbion* in a lophophorate–aschelminth–protostome clade together with annelids, molluscs, rotifers, acanthocephalans, phoronids, brachiopods, ectoprocts, entoprocts, pogonophorans, vestimentiferans and echiurans (not shown). As this data set was too large to apply other reconstruction methods and stability tests, all further analyses were restricted to a data set of 36 taxa belonging to Arthropoda or to the lophophorate– aschelminth–protostome clade (Fig. 1). All reconstructions, for which the results are combined in a strict consensus tree (Fig. 1), show significant support for a sister-group relationship of Cycliophora to Rotifera and Acanthocephala. In agreement with previous findings[9–11], our analyses indicate that Acanthocephala is a subgroup of the Rotifera.

Our neighbour-joining analyses indicated that *Philodina acuticornis* and *Moliniformis moliniformis* are long branches, which may produce artificial groupings. Excluding both species did not affect the significantly supported nodes of Fig. 1 and resulted in only a small increase in the maximum parsimony consistency index (to 0.393). Therefore, it is unlikely that these long branches caused topological errors in our trees. Hence, the clustering of *P. acuticornis* and *M. moliniformis* is probably not an artefact.

The protostome affinities of Cycliophora are consistent with morphological data[1,2]. *Symbion* has been tentatively proposed to be a sister group to Entoprocta. However, it also shares similarities with Ectoprocta and some aschelminth phyla[2]. The 18S rRNA data do not provide evidence to suggest that cycliophorans may be neotenic entoprocts, but do indicate a relationship to Rotifera and Acanthocephala. Such a relationship was previously rejected[1,2], despite some morphological support. Both rotifers and cycliophorans have dwarf males and hypodermic insemination. As in sessile rotifers, the digestive tract of cycliophorans is U-shaped and the anus is located in the neck region outside the buccal funnel (the anus of sessile rotifers is located outside the corona). The digestive tract of entoprocts is U-shaped, too, but the anus is located inside the tentacular crown.

Moreover, the monophyly of the clade comprising Rotifera, Acanthocephala and Cycliophora is further supported by the common presence of protonephridia with multiciliated terminal cells. The plesiomorphic (or primitive) condition is one cilium per terminal cell, which is found in Gnathostomulida, Loricifera and some Priapulida. Kinorhyncha and several Priapulida have two cilia per cell. The apomorphic (or derived) condition is the presence of many cilia per terminal cell as in Rotifera, Acanthocephala and now Cycliophora. Protonephridia are lacking in Ectoprocta, but are present in Entoprocta. Finally, some rotifers (for example, *Seison* and *Embata*[12]) have also adopted commensalistic lifestyles on crustacean gills.

Although the Cycliophora have several striking similarities with sessile rotifers, there is no evidence that they should be included as a subtaxon in Rotifera. The separate status of Cycliophora is supported by differences present in the cuticle and by the lack of a mastax, a feature always present in Rotifera. Both Acanthocephala and Rotifera have an intracellular matrix layer and the epidermal cells consist of a syncytium, whereas *Symbion* has a true cuticle formed by normal epidermal cells. Owing to the basal position of *Symbion* in the Acanthocephala–Rotifera–Cycliophora clade, it is unlikely that the mastax has been secondarily lost in Cycliophora, as it has in the Acanthocephala.

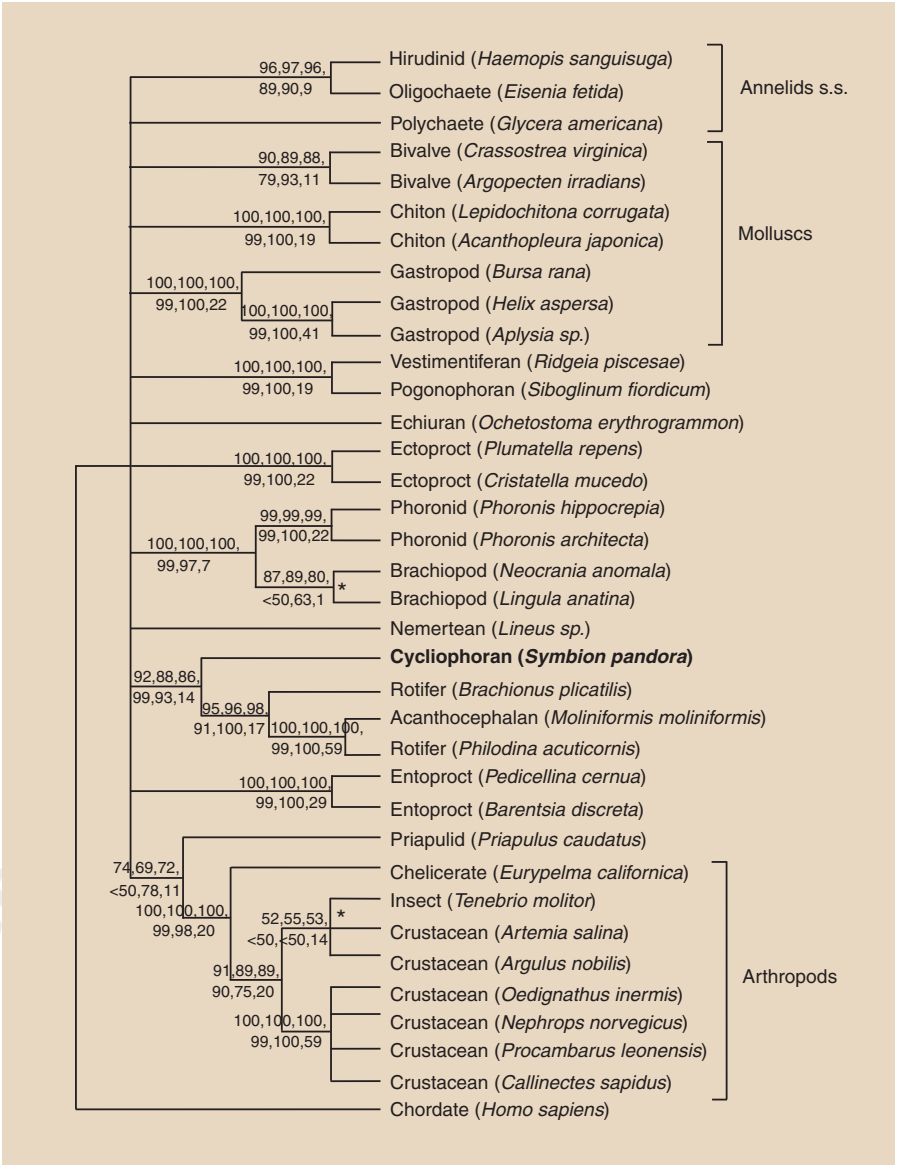

Figure 1 Strict consensus tree, showing groups present in all trees obtained by four different tree-construction methods applied to an 18S rRNA data set[6] that includes the *S. pandora* and *N. norvegicus* data. Methods used were maximum parsimony analysis (two maximum parsimony trees, 3,850 steps, consistency index 0.383) and neighbour-joining analysis on the basis of Kimura[13], Jukes–Cantor[14] or substitution-rate-calibration[15] distances. Numbers at nodes are, respectively, bootstrap values of these four methods, confidence probability values[7] and decay indices[8]. All values are percentages, except for decay indices (number of extra steps for a clade not to be unequivocally supported). Nodes marked by asterisks were altered by removing long branches *P. acuticornis* and *M. moliniformis*.

B. M. H. Winnepenninckx, T. Backeljau
Royal Belgian Institute of Natural Sciences, Vautierstraat 29, B-1000 Brussels, Belgium
e-mail: birgitta@uia.ua.ac.be
R. M. Kristensen
Zoological Museum, University of Copenhagen, Universitetsparken 15, DK-2100 Copenhagen, Denmark

1. Funch, P. & Kristensen, R. M. *Nature* **378,** 711–714 (1995).
2. Funch, P. & Kristensen, R.M. in *Microscopic Anatomy of Invertebrates 13: Lophophorates, Entoprocta and Cycliophora* (eds Harrison, F.W. & Woollacott, R.M.) 409–474 (Wiley-Liss, New York, 1997).
3. Funch, P. *J. Morphol.* **230,** 231–263 (1996).
4. Conway Morris, S. *Nature* **378,** 661–662 (1995).
5. d'Hondt, J.-L. *Bull. Mens. Soc. Linn. Lyon* **66,** 12–22 (1997).
6. Van de Peer, Y., Caers, A., De Rijk, P. & De Wachter, R. *Nucleic Acids Res.* **26,** 179–182 (1998).
7. Kumar, S., Tamura, K. & Nei, M. *MEGA: Molecular Evolutionary Genetics Analysis Version 1.0: Manual* (Pennsylvania State Univ., Pennsylvania, 1993).
8. Bremer, K. *Evolution* **42,** 795–803 (1988).
9. Lorenzen, S. in *The Origins and Relationships of Lower Invertebrates* (eds Conway Morris, S., George, J. D., Gibson, R. & Platt, H. M.) 210–223 (Clarendon, Oxford, 1985).
10. Garey, J. R., Near, T. J., Nonnemacher, M. R. & Nadler, S. A. *J. Mol. Evol.* **43,** 287–292 (1996).
11. Ahlrichs, W. H. *Zoomorphology* **117,** 41–48 (1997).
12. Brusca, R. C. & Brusca, G. J. *Invertebrates* (Sinauer, Sunderland, 1990).
13. Kimura, M. *J. Mol. Evol.* **16,** 111–120 (1980).
14. Jukes, T. H. & Cantor, C. R. in *Mammalian Protein Metabolism* (ed. Munro, H. N.) 21–132 (Academic, New York, 1969).
15. Van de Peer, Y., Van der Auwera, G. & De Wachter, R. *J. Mol. Evol.* **42,** 201–210 (1996).

Gulf Stream shifts following ENSO events

Over the past three decades the annual mean latitude of the Gulf Stream off the coast of the United States has been forecastable from the intensity of the North Atlantic Oscillation (NAO)[1], the predictions accounting for more than half the variance. Here we show that much of the unexplained variance can be accounted for by the Southern Oscillation in the Pacific, the Gulf Stream being displaced northwards following El Niño–Southern Oscillation (ENSO) events. This provides a link between events in the equatorial Pacific and the circulation and weather conditions of the North Atlantic.

Monthly charts showing the position of the north wall of the Gulf Stream since 1966 have been used to study its long-term variations[2,3] and to construct an index of its latitude by principal components analysis[1]. Ocean circulation theory predicts that the path of the Gulf Stream is set by the line of zero Ekman pumping, where there is no wind-driven convergence or divergence of water at the ocean surface[4]. The position of the Gulf Stream will therefore vary with the intensity of the North Atlantic Oscillation, the dominant mode of mid-latitude atmospheric variation in the North Atlantic, and indeed 60% of the annual variance in the latitude of the north wall 1966–96 is predictable from an NAO index[1,5].

Another source of fluctuation in the Gulf Stream is the subtropical and tropical trade wind belt. This is a region that is strongly affected by ENSO events in the Pacific Ocean, their influence appearing in African weather patterns[6]. Figure 1a shows that the residuals from a multiple regression prediction of the Gulf Stream position based on the NAO index are correlated with the values from two years earlier of one measure of ENSO variations, the September-to-February averages of the Southern Oscillation (SO) index (the difference in sea-level pressure anomalies between Tahiti and Darwin). The SO index is uncorrelated with the NAO index[7].

We used a stepwise regression analysis to relate the annual Gulf Stream position during 1966–97 to the previous year's position (to take account of persistence between years) and the NAO and SO indices at lags of up to two years. For each of these indices, the largest and most significant contribution was made by the value of the index from two years previously, there being no significant contributions from the NAO and SO index at a one-year lag or from the unlagged SO index. The predictions of the regression equation (F-ratio = 22.7, $P < 0.01$) are shown in Fig. 1b. The two-year time lag is consistent with an earlier study of the latitude at which the Gulf Stream separates from the coast of the United States. Gangopadhyay *et al.*[4] found that the theoretically predicted latitudes during 1977–88 only agreed with those observed if the wind forcing was integrated over about three years, a delay they attributed to the adjustment time of the ocean circulation.

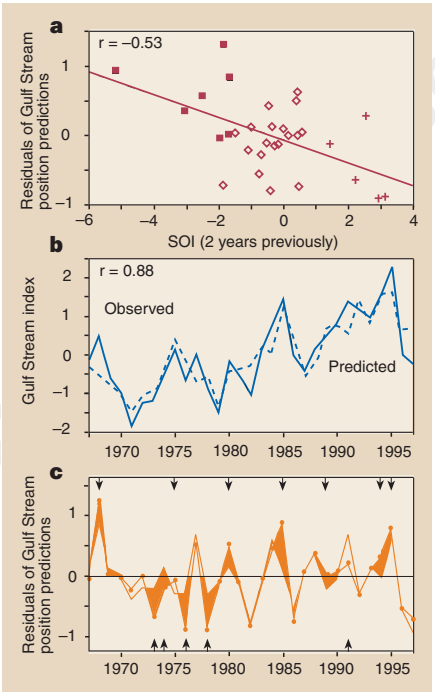

Figure 1 Observed and predicted Gulf Stream positions. **a,** Scatter plot comparing observed and predicted Gulf Stream positions (1966–97)[1] with the SO index two years previously (index has been allocated to the year of the January data). The prediction was based on a multiple regression equation using the NAO index[5] and its value two years before, and the previous year's position. A regression line through the points is shown. Filled squares, the El Niño years (1966, 1973, 1978, 1983, 1987 and 1992–93); crosses, the La Niña years (1971–72, 1974, 1976 and 1989); diamonds, years belonging to neither group. **b,** Latitude of Gulf Stream 1966–97 (solid line) compared with the predictions of the regression equation (broken line) in which the delayed effect of the SO is added to the variables in **a**. The units of the index are equivalent to 0.03° at 79° W and 0.3° at 65° W. **c,** Reduction of regression residuals when delayed effect of the SO is considered (filled circles, original regression results). Downward arrows, two years after an El Niño; upward arrows, two years after a La Niña. Shaded regions, associated reductions of residuals. Correlation coefficients (r) both have $P < 0.01$. (All significance levels corrected for lag 1 serial correlation[11].)

Because of intercorrelation between the variables, it is not possible to obtain a unique value for the contribution of the SO index to the predictions in Fig. 1b. Thus the stepwise regression indicates that the index accounts for 9% of the variance, but the partial correlation coefficient between the Gulf Stream index and the SO index is 0.4, which indicates that the percentage could be larger. Figure 1c shows how including the lagged SO index reduces the regression residuals: after El Niño or La Niña events, the residual is reduced in the direction of the arrows.

Averaging the data from ref. 1 over the region from 65° to 79° W shows that the mean latitude of the Gulf Stream two years after ENSO events was 0.2° further north than after non-event years ($P < 0.001$). These displacements represent two-thirds of a standard deviation (the southward shift following La Niña events, 0.05°, was not significant). The displacements may be accompanied by larger shifts further east, where the Stream's path is less constrained, or by more substantial circulation changes elsewhere.

The position of the Gulf Stream affects the waters over the continental shelf from Cape Hatteras to the Grand Banks in several ways[8] and may influence storm tracks over the northwest Atlantic[9,10] The results in Fig. 1 indicate that these processes may be linked to ocean–atmosphere events in the tropical Pacific.

Arnold H. Taylor, Michael B. Jordan, John A. Stephens

NERC Centre for Coastal and Marine Sciences, Plymouth Marine Laboratory, Prospect Place, West Hoe, Plymouth PL1 3DH, UK

e-mail: aht@pml.ac.uk

1. Taylor, A. H. & Stephens, J. A. *Tellus* **50 A,** 134–142 (1998).
2. Miller, J. L. *J. Geophys. Res.* **99,** 5057–5064 (1994).
3. Drinkwater, K. F., Myers, R. A., Pettipas, R. G. & Wright, T. L. *Can. Data Rep. Hydrogr. Ocean Sci.* **125,** 1–103 (1994).
4. Gangopadhyay, A., Cornillon, P. & Watts, R. D. *J. Phys. Oceanogr.* **22,** 1286–1301 (1992).
5. Hurrell, J. W. *Science* **269,** 676–679 (1995).
6. Cane, M. A., Eshel, G. & Buckland, R. W. *Nature* **370,** 204–205 (1994).
7. Rogers, J. C. *Mon. Weath. Rev.* **112,** 1999–2015 (1984).
8. Myers, R. A. & Drinkwater, K. F. *J. Mar. Res.* **47,** 635–656 (1989).
9. Dickson, R. R. & Namias, J. *Mon. Weath. Rev.* **104,** 1255–1265 (1976).
10. Cione, J. J., Raman, S. & Pietrafesa, L. J. *Mon. Weath. Rev.* **121,** 421–430 (1993).
11. Taylor, A. H. *ICES J. Mar. Sci.* **52,** 711–721 (1995).